The aerobic respiratory chain of the acidophilic archaeon Ferroplasma acidiphilum: A membrane-bound complex oxidizing ferrous iron

ARTICLE *in* BIOCHIMICA ET BIOPHYSICA ACTA · APRIL 2015

Impact Factor: 4.66 · DOI: 10.1016/j.bbabio.2015.04.006 · Source: PubMed

Biochimica et Biophysica Acta 1847 (2015) 717–728

Contents lists available at ScienceDirect

Biochimica et Biophysica Acta

journal homepage: www.elsevier.com/locate/bbabio

The aerobic respiratory chain of the acidophilic archaeon *Ferroplasma acidiphilum*: A membrane-bound complex oxidizing ferrous iron

Cindy J. Castelle [a,1], Magali Roger [a], Marielle Bauzan [b], Myriam Brugna [a], Sabrina Lignon [c], Manfred Nimtz [d], Olga V. Golyshina [d,e], Marie-Thérèse Giudici-Orticoni [a], Marianne Guiral [a,*]

[a] CNRS, Aix Marseille Université, BIP UMR 7281, FR 3479, 13402 Marseille, France
[b] CNRS, Aix Marseille Université, Unité de Fermentation, FR 3479, 13402 Marseille, France
[c] CNRS, Aix Marseille Université, Plate-forme Protéomique MaP IBiSA, FR 3479, 13402 Marseille, France
[d] Helmholtz Centre for Infection Research, 7 Inhoffen Strasse, 38124 Braunschweig, Germany
[e] School of Biological Sciences, Deiniol Road, LL57 2UW, Bangor, UK

ARTICLE INFO

Article history:
Received 19 November 2014
Received in revised form 7 April 2015
Accepted 12 April 2015
Available online 18 April 2015

Keywords:
Ferroplasma
Acidophilic archaea
Iron oxidation pathway
Cytochrome oxidase
Sulfocyanin
Cytochrome *ba* complex

ABSTRACT

The extremely acidophilic archaeon *Ferroplasma acidiphilum* is found in iron-rich biomining environments and is an important micro-organism in naturally occurring microbial communities in acid mine drainage. *F. acidiphilum* is an iron oxidizer that belongs to the order *Thermoplasmatales* (*Euryarchaeota*), which harbors the most extremely acidophilic micro-organisms known so far. At present, little is known about the nature or the structural and functional organization of the proteins in *F. acidiphilum* that impact the iron biogeochemical cycle. We combine here biochemical and biophysical techniques such as enzyme purification, activity measurements, proteomics and spectroscopy to characterize the iron oxidation pathway(s) in *F. acidiphilum*. We isolated two respiratory membrane protein complexes: a 850 kDa complex containing an aa_3-type cytochrome oxidase and a blue copper protein, which directly oxidizes ferrous iron and reduces molecular oxygen, and a 150 kDa cytochrome *ba* complex likely composed of a di-heme cytochrome and a Rieske protein. We tentatively propose that both of these complexes are involved in iron oxidation respiratory chains, functioning in the so-called uphill and downhill electron flow pathways, consistent with autotrophic life. The cytochrome *ba* complex could possibly play a role in regenerating reducing equivalents by a reverse ('uphill') electron flow. This study constitutes the first detailed biochemical investigation of the metalloproteins that are potentially directly involved in iron-mediated energy conservation in a member of the acidophilic archaea of the genus *Ferroplasma*.

1. Introduction

Iron oxidation pathways in micro-organisms are important components of the iron geochemical cycle. Organisms that are able to oxidize ferrous iron (Fe(II)) to ferric iron (Fe(III)) are widespread on the microbial phylogenetic tree and thrive in a wide variety of environments such as pyrite ores, acid springs, freshwater sediments, plant rhizospheres or marine hydrothermal vents. Some of these organisms are acidophilic bacteria or archaea and have an optimum pH for growth of less than 3. An important aspect of acidophiles lies in their biotechnological application for metal extraction from acid drainage produced during the mining of ores (bioleaching) [1–3]. The bacterium *Acidithiobacillus ferrooxidans* uses Fe(II) as electron donor for growth and is by far the best characterized acidophilic iron-oxidizing prokaryote [4–8]. Investigations of microbial iron oxidation, especially at the molecular level, have lagged behind studies of pathways utilizing other inorganic sources of energy. With the exception of *Acidithiobacillus*, only fragmentary data are available on the metabolic processes occurring in iron-oxidizing micro-organisms, as reviewed in [7–9]. This is due in part to the low growth yields of Fe-oxidizing micro-organisms and the lack of genetic tools developed for these species.

The genus *Ferroplasma* is proposed to be a part of the family *Ferroplasmaceae* within the order *Thermoplasmatales*, but it shares several metabolic aspects with other archaeal species of the order *Sulfolobales* as well as with the bacteria of the genera *Acidithiobacillus* and *Leptospirillum*. *Ferroplasma* is found in sulfide ore deposits around the globe and is probably one of the major players in the biogeochemical cycling of sulfur and sulfides in highly acidic environments, thus constituting an ideal model for biochemical investigations [10,11]. Moreover, members of the *Ferroplasmaceae*, along with the *Picrophilaceae*, are the most extremely acidophilic micro-organisms known so far. The genus *Ferroplasma* is represented by one species with the validated

Abbreviations: Bis-tris, 2,2-Bis(hydroxymethyl)-2,2′,2″-nitrilotriethanol; BN gel, Blue-native gel; DDM, Dodecyl-β-D-Maltoside; 2D, two-dimensional.

* Corresponding author at: Laboratoire de Bioénergétique et Ingénierie des Protéines (UMR 7281), CNRS-Aix-Marseille université, 31 chemin Joseph Aiguier, 13402 Marseille cedex 20, France. Tel.: +33 4 91 16 44 04; fax: +33 4 91 16 40 97.
E-mail address: guiral@imm.cnrs.fr (M. Guiral).
[1] Present address: Department of Earth and Planetary Science, 307 McCone Hall University of California, Berkeley, CA 94720, United States.

http://dx.doi.org/10.1016/j.bbabio.2015.04.006
0005-2728/

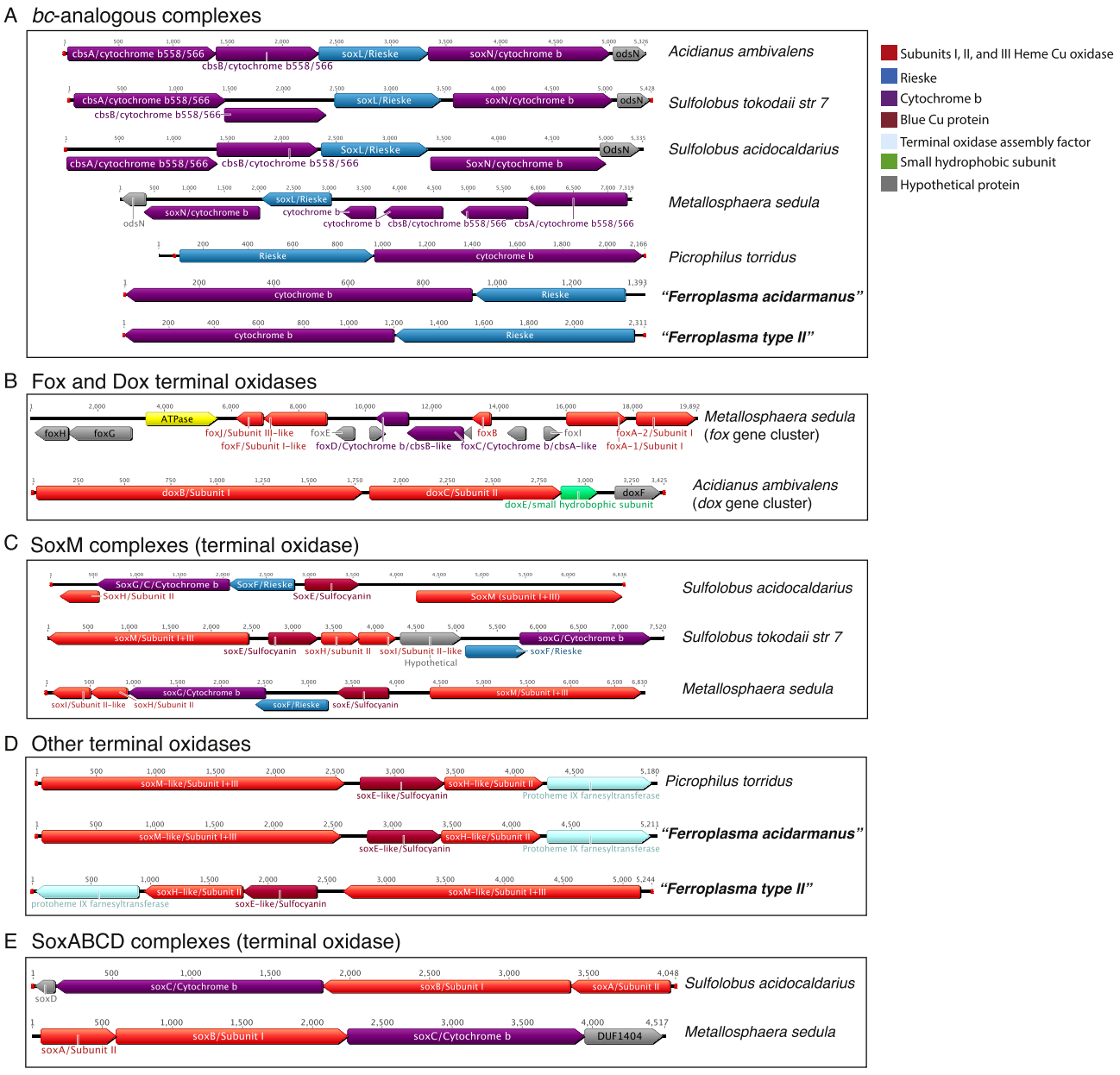

Fig. 1. Genes and surrounding regions of the terminal oxidases and *bc*-analogous complexes from various archaea. A, *bc*-analogous complexes; B, Fox and Dox terminal oxidases; C, SoxM terminal complexes; D, Other terminal oxidases related to the SoxM complex. Subunit I + III corresponds to a fusion of subunits I and III of heme/copper-type cytochrome oxidase. The *Ferroplasma* terminal oxidase enzyme is made of two subunits and is an A-type oxygen reductase that possesses the CuA binding site in subunit II [29,30]. The last gene of the oxidase operons encodes a putative prenyltransferase and has homologies with the protoheme IX farnesyltransferase, enzyme involved in heme biosynthesis; E, SoxABCD complexes. Gene clusters were organized and visualized using Geneious v7.0.6.

name *F. acidiphilum* [12], whereas two other *Ferroplasma*-like organisms named "*Ferroplasma acidarmanus*" and "*Ferroplasma thermophilum*" were previously described [1,13,14], all three strains using Fe(II) to grow. The genome of "*F. acidarmanus* fer1" is almost completely sequenced [15] as well as the metagenome of "*Ferroplasma* sp. Type II" [16]. *F. acidiphilum* (strain Y^T, DSMZ 12658) is a slow-growing, cell wall-less, acidophilic (optimum pH for growth of 1.7) and mesophilic archaeon isolated from a pyrite-leaching pilot plant. It oxidizes Fe(II) as its sole energy source and fixes inorganic carbon [12]. Although *Ferroplasma* archaea are abundant in the environment, very little is known about the respiratory chain of these iron-oxidizers. A putative electron transport chain has been suggested for "*F.* Type II", based exclusively on metagenome sequence analysis. Its constituent redox proteins are proposed to assemble into a supercomplex similar to the SoxM or SoxM-like supercomplexes found in the hyperthermoacidophilic non-iron oxidizing archaeal *Sulfolobus* species [17–25]. These unusual archaeal Sox supercomplexes combine structural elements from both bc_1 complexes and classical terminal oxidases. The corresponding operons and their gene product characteristics are presented in Figs. 1 and S1 (Supporting information). For "*F. acidarmanus* fer1", preliminary data (electron transport chain inhibition studies, spectroscopy analysis and proteomic results) on whole cells or on membrane fragments suggest that Fe(II) oxidation is mediated by a blue copper protein sharing sequence characteristics with rusticyanin and sulfocyanin (SoxE) from *Acidithiobacillus* and *Sulfolobus* respectively, and that the derived electrons pass to a terminal oxidase [26] (Figs. 1 and S1). In heterotrophic growth, reduced carbon molecules allow the production of NADH, which in turn reduces the quinone pool. In mixotrophic growth, Fe(II) is assumed to be oxidized by sulfocyanin (Fig. S1). Although "*F. acidarmanus*" and *F. acidiphilum* are related, their lifestyle may be different. Indeed,

F. acidiphilum is able to fix CO_2, a trait not shared by "*F. acidarmanus*" which is described as mixotrophic or heterotrophic, rendering the investigation of the *F. acidiphilum* respiratory machinery fundamental for a better understanding of its physiology.

Motivated by (i) the lack of a detailed picture of aerobic iron oxidation in archaea, (ii) their involvement in natural and biotechnological leaching processes, and (iii) the exceptional physiological and metabolic properties of *F. acidiphilum*, we investigated the biochemistry of iron oxidation and oxygen reduction in this archaeon to characterize its iron respiratory system at the molecular level. This work led us to identify and characterize two respiratory membrane protein complexes, and thus obtain a clearer picture of the components involved in respiration in *Ferroplasma*.

2. Materials and methods

2.1. Growth conditions

F. acidiphilum DSM 12658 was grown on the medium DSM 874 in 20 L glass bottles at 37 °C, pH 1.7, as described by Golyshina et al. [12]. The cultures were aerated with an airflow of 10 L/min (0.5 volume of air per volume of medium per minute) and stirred at 250 rpm on a magnetic stirrer. After 96 h of growth, cells were pelleted using a continuous centrifugation system (Sharples T1) at 20,000 ×*g*, washed twice with fresh medium (without iron) to remove iron, frozen in liquid nitrogen and stored at −80 °C until further analysis. Per L of culture, 150 mg of cells (wet weight) was obtained.

2.2. Preparation and solubilization of membranes

Cells (4–5 g) were resuspended in 15–20 mL of 50 mM Bis-tris pH 7 (buffer A) or 100 mM of sodium citrate pH 3 (buffer B) supplemented with protease inhibitors and with DNase I 10 μg mL^{-1} (Roche). The cells were broken at 18–20,000 PSI using a French press cell. Membranes were pelleted by centrifugation at 145,000 ×*g* for 1 h at 4 °C and resuspended in buffer A or buffer B, both containing 5% (v/v) glycerol and 750 mM aminocaproic acid to give a protein concentration of about 10 mg mL^{-1}. Membranes were solubilized with Dodecyl-β-D-Maltoside (DDM) at a ratio of 3 mg DDM/mg of proteins at either pH 7 or pH 3. Solubilization was allowed to proceed for 3 h at 4 °C, under gentle shaking. Unsolubilized material was pelleted by ultracentrifugation at 200,000 ×*g* for 1 h 15. Samples were concentrated using Vivaspin ultrafiltration spin columns of 100,000 MWCO (Sartorius). Protein concentration was determined with the Bicinchoninic Acid Protein Assay Kit (Sigma) using Bovine Serum Albumin as standard.

2.3. Purification of protein complexes

For the purification of the 850 kDa and 370 kDa complexes, concentrated solubilized membrane proteins (obtained at pH 3) were layered on top of a 15–40% glycerol gradient (43 mL) formed in buffer B containing 0.1% DDM, and centrifuged at 145,000 ×*g* overnight at 4 °C. Fractions 1 to 6 (F1 to F6, 7 mL each) were collected starting from the top of the tube and concentrated. The densest fraction of glycerol gradient (35–40%) was concentrated and then applied to a Superose 6 gel filtration column (FPLC, GE Healthcare, 25 mL), equilibrated with buffer B and 0.01% DDM, at a flow rate of 0.2 mL min^{-1}. Fractions (0.5 mL) with specific spectroscopic signals of cytochromes and cytochrome *c* oxidase were pooled and concentrated. For the enrichment of the 150 kDa cytochrome b_{562}–a_{582} complex, fractions F2 and F3 from the glycerol gradient were pooled and applied to a hydroxyapatite column equilibrated with 50 mM sodium acetate pH 5, 0.01% DDM and 5% glycerol. Fractions displaying signals at 562 nm (cyt *b*) and 582 (cyt *a*) nm in optical spectra were eluted between 250 and 500 mM potassium phosphate.

2.4. Separation by Blue native gel electrophoresis

Blue native (BN) gels were performed as previously described [27]. Gels were stained with Coomassie Brilliant Blue R-250 or enzyme activities were revealed. Protein bands were excised from gels and stored at −20 °C until further analysis by mass spectrometry.

2.5. In-gel enzyme activity measurements

Cytochrome *c* oxidase activity was revealed in the gel using horse heart cytochrome *c* and diaminobenzidine, as described by Guiral et al. [27], except that the pH was 6.8. In the current work, an assay was developed for the detection of iron oxidase activity (electron transfer from Fe(II) to oxygen) in BN gels via incubation in a solution of 10 mM $FeSO_4$ and 50 mM glycine at pH 3. Negative control experiments were performed using 1 mM potassium cyanide (KCN) in the reaction medium or in semi-anaerobic conditions by bubbling the reaction buffer with argon gas before addition of reactants. All activity measurements were done at room temperature.

2.6. Separation by 1D-SDS and 2D-SDS/BN electrophoresis

Proteins were separated on 1D SDS gels as previously described [27]. For the second dimension, a 1.5 mm thick denaturing gel containing 15% acrylamide with no stacking gel was used. After migration, proteins were revealed with Coomassie Brilliant Blue. Protein bands were cut out from gels and stored at −20 °C for later mass spectrometry analysis.

2.7. Activity measurements

For the measurement of cytochrome *c* oxidase activity, the oxidation rate of horse heart ferrocytochrome *c* (50 μM) was monitored spectrophotometrically at 552 nm in 20 mM ammonium acetate at pH 5, in the presence or absence of 300 μM KCN. The cytochrome oxidation rate was calculated using the slope of the straight line-part of the graph with the molecular extinction coefficient of horse cytochrome *c* $\varepsilon_{550\ nm} = 29\ mM^{-1}\ cm^{-1}$. One unit of cytochrome *c* oxidase activity corresponds to the oxidation of 1 nmol of cytochrome *c*/min.

Oxygen consumption by purified complexes containing the cytochrome *c* oxidase (50 μg) was also measured polarographically with a Clark electrode (Gilson oxygraph). This was done in buffer B with Fe(II) as electron donor in a 1.8 mL reaction vessel. Fe(II) oxidase activity was started by the addition of 28 mM $FeSO_4$. When used, KCN was added at a final concentration of 300 μM. One unit of Fe(II) oxidase activity corresponds to the consumption of 1 nmol of O_2/min. All activities assays were done in triplicate at room temperature.

2.8. Spectroscopy

UV–Visible spectra were recorded with a Cary 50 Bio (Varian) spectrophotometer at room temperature. Samples were analyzed "as prepared" (untreated) or reduced with sodium ascorbate or sodium dithionite. EPR spectra were recorded at liquid helium temperatures with a Bruker ESP 300e X-band spectrometer equipped with an Oxford Instruments cryostat and temperature control system. Spectra were recorded on "as prepared" samples at a total protein concentration of 17 mg mL^{-1}. Instrument settings were as follows: temperature, 15 K; microwave frequency, 9.406 GHz; microwave power, 6.4 mW; and modulation amplitude, 3 mT. Sixteen scans were averaged for each spectrum.

2.9. Mass spectrometry identification

For native gel samples, a robotic workstation (Freedom EVO 100, TECAN) was used to perform automated sample preparation, including multiple steps: washes, reduction and alkylation, digestion by trypsin

(PROMEGA, proteomics grade with 0.025% ProteasMAX™) and extraction of tryptic peptides. Samples were then analyzed on a LCQ Deca^{XP+} mass spectrometer (Thermo Fisher) coupled to a liquid chromatography system (Finnigan Surveyor HPLC) as previously described [27]. Spectra were processed by Bioworks 3.3 software and the identification protein search was both performed by Mascot (in situ license) and Sequest, using the following parameters: NCBI database reduced to "*F. acidarmanus*" fer1 and Type I, *Picrophilus torridus* DSM 9790, *Thermoplasma acidophilum* DSM 1728, *Thermoplasma volcanium* GSS1, "*Candidatus* Micrarchaeum *acidiphilum*" ARMAN-2, *Sulfolobus tokodaii* str. 7, *Acidianus ambivalens* (21,279 entries including the human keratins and the trypsin), variable modifications: Carbamidomethylation (C), Oxidation (M), 2 missed cleavages, Mass Tolerance: ±1.5 Da, Fragment Mass Tolerance: ±0.8 Da. As the genome of *F. acidiphilum* is not available, proteins were considered as identified in both search engines by 1 unique peptide with ion significance threshold or at least 5 consecutive b and y ion fragments.

Proteins from SDS gel samples were identified by ESI-Tandem MS analysis of tryptic peptides. The protein bands were excised from gels, dried, reduced and carboxamidomethylated followed by digestion with trypsin. The resulting peptides were extracted and purified according to standard protocols. A Q-ToF II mass spectrometer (Micromass, UK) equipped with a nanospray ion source and gold-coated capillaries was used for electrospray ionization (ESI) MS of peptides. For collision-induced dissociation experiments, multiple charged precursor ions were selectively transmitted from the quadrupole mass analyzer into the collision cell (25–30 eV). The resulting fragment ions were separated by an orthogonal time-of-flight mass analyzer. The acquired MS/MS spectra were further enhanced (Max. Ent. 3; Micromass) and used for manual de novo sequencing of the tryptic peptides. The obtained amino acid sequences were used for homology searches in public primary protein sequence databases (http://blast.ncbi.nlm.nih.gov/Blast.cgi?PROGRAM=blastp&BLAST_PROGRAMS=blastp&PAGE_TYPE=BlastSearch&SHOW_DEFAULTS=on&LINK_LOC=blasthome).

2.10. ORF prediction

Geneious software v7.1.7 [28] was used to predict putative ORFs in the archaeal genomes described in this study.

3. Results

3.1. Genome analysis of potential iron oxidizing pathway operons in Ferroplasma and comparison with other acidophilic archaea

In bacteria, iron oxidation pathways are mostly comprised of *c*-type cytochromes, copper or iron–sulfur proteins and terminal oxidases [8]. Electron transport from iron to oxygen is much less studied in archaea. In *Sulfolobales* (*Metallosphaera* and *Sulfolobus* species), it is predicted to be associated with redox proteins encoded by the large *fox* operon (for *f*errous iron *ox*idation). This operon includes a *b*-type cytochrome assumed to be the direct oxidant of ferrous iron, an iron–sulfur protein, a multicopper protein and a terminal heme copper oxidase [8,31,32] (Fig. 1B). The *sox*NL-*cbs*AB operon encodes components important for iron utilization in *Metallosphaera* (Fig. 1A), but is also present in archaea not capable of iron oxidation (such as *A. ambivalens*). Such *fox* and *sox-cbs* operons are missing in the genomic or metagenomic sequences of *Ferroplasma* species, as well as the *pio* or *rus* operons essential for iron oxidation in bacteria [8,33]. In *Thermoplasmatales*, only two putative iron oxidation operons are found, one encoding a putative SoxM-like terminal oxidase (with genes for subunits I + III fused and subunit II and for a sulfocyanin, Fig. 1D) and one encoding a putative *bc*-analogous complex (with genes for a Rieske iron–sulfur protein and a cytochrome *b*, Fig. 1A). Both of these operons differ in terms of composition from those found in acidophilic archaea, whether they are iron-oxidizers or not (Fig. 1). It was previously proposed, on the basis of comparative genomics and structural modeling, that the heme copper oxidase of *Ferroplasma* (Fig. 1D) belongs to the A-family (along with SoxM, but in a different subfamily), whereas SoxB, Dox and Fox are included in the E-, D- and F-family, respectively [34]. The Fox, Dox, Sox-Cbs, SoxM or SoxB complexes seem to be absent in *Ferroplasma* (Fig. 1). The bioenergetic pathways of *Ferroplasma* thus appear to be simpler compared to some other archaea for which a large number of respiratory complex operons are present in the genome (for instance five different terminal oxidases in *Metallosphaera yellowstonensis*). Biochemical approaches appear to be essential to characterize the respiratory complexes in *Ferroplasma* and determine their role in the iron oxidation pathway.

3.2. Spectroscopic characterization of F. acidiphilum membrane protein complexes

To identify the proteins involved in the Fe(II) oxidation/O_2 reduction pathway and study its organization, we prepared and solubilized membranes from *F. acidiphilum* cells using 2% DDM (Dodecyl-β-D-Maltoside) at pH 3 and pH 7. Finding the optimal pH for membrane enzyme activities and stability is a relevant issue because depending on their orientation in the membrane, the proteins may be exposed either to the external environment at pH 2 or to the nearly neutral pH of the cytoplasm [35]. Optical spectra of sodium dithionite-reduced solubilized membranes, recorded at room temperature, showed absorption peaks in the α-band region at 562, 582 and 597 nm (Fig. 2A and B). A small peak at 531 nm is also visible at pH 3. These signals suggest the presence of *a*- and *b*-type cytochromes. This is confirmed by signals in the Soret region at 417 and 430 nm in the "as prepared" samples, and at 430 nm with a shoulder at 440 nm in the reduced samples. These spectra are similar to those published for membranes of *S. tokodaii* (previously named sp strain 7) and *Sulfolobus acidocaldarius* [20,24,36], and have features found in "*F. acidarmanus*" membrane spectra [26] (Table 1).

As shown in previous studies, terminal oxidase supercomplexes or cytochrome-harboring complexes of archaeal respiratory chains contain *a*-type cytochromes that exhibit unusual absorbance peaks at 582–587 nm [17,25,41]. This is probably linked to an unusual environment of the heme *a* in these proteins [20]. So far, this type of heme has been mostly found in archaeal proteins that show a clear sequence similarity to di-heme cytochrome *b* (Table 1, Fig. S1). In *F. acidiphilum* samples, we thus attribute the peak observed at 582 nm to heme(s) a_{582}. The absorption peaks at 430, 531 and 562 nm are typical of cytochrome *b* hemes, for instance the cytochrome b_{562} associated with electron transport complexes in *Sulfolobus* species [18,19]. Signals at 440 and 597 nm (Fig. 2A and B) point to the presence of *a*-type hemes in solubilized *Ferroplasma* membranes, likely as part of the terminal heme copper oxidase (Fig. 1D). This terminal oxidase is possibly of the aa_3-type such as that reported for acidophilic archaea including *S. tokodaii*, *S. acidocaldarius* (SoxABCD complex) and *A. ambivalens* [44] (Table 1 and Fig. S1), and the non-acidophilic archaeon *Haloferax volcanii* [47]. Alternatively, the presence of a ba_3 oxidase in *F. acidiphilum* may be considered since a signal at 562 nm is also detected (as in the SoxM complex of *S. acidocaldarius*, Fig. S1 and Table 1). All in all, these optical spectra indicate that complexes containing hemes a_{582}, b_{562} and a/a_3 have been solubilized from *F. acidiphilum* membranes. They are likely encoded by genes included in the operons depicted in Fig. 1A and D, and probably correspond to a terminal oxidase and a *bc*-analogous complex or to a supercomplex resulting from the interaction of both complexes.

Optical spectra done with membranes obtained at pH 3 and 7 show similar absorbance characteristics. Spectral differences between cytochromes at different pH were observed previously [20], which may be rationalized by some metalloproteins being sensitive to acidification of the archaeal cell membranes. However, in our samples no blue-shift of

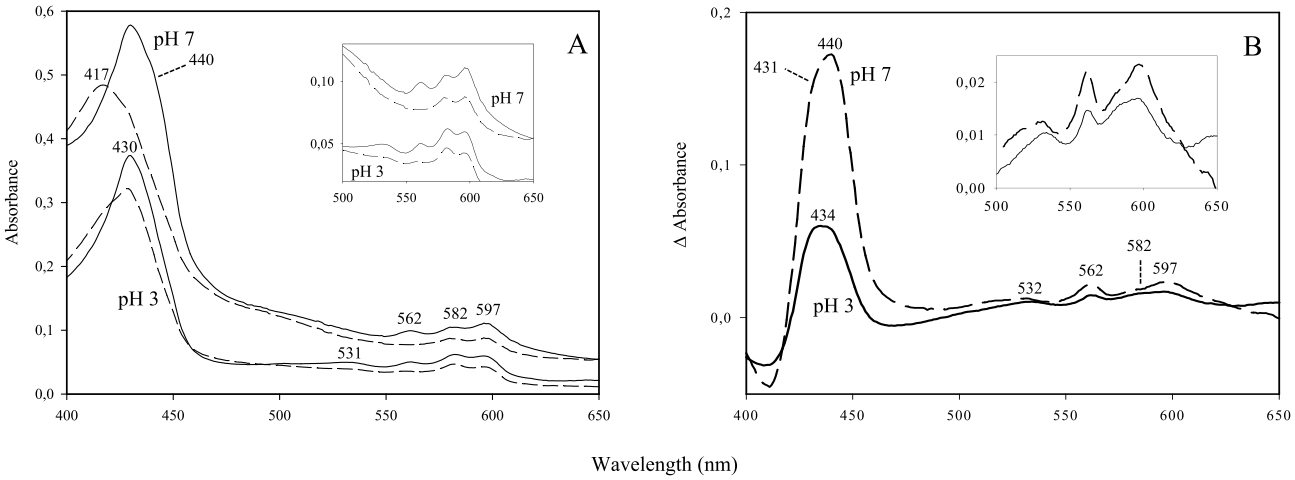

Fig. 2. Absorption spectra of solubilized membranes from *Ferroplasma acidiphilum*. A, Solubilized membranes at pH 3 and pH 7 were analyzed "as prepared" (dashed lines) and reduced by sodium dithionite (solid lines). B, Difference spectra (reduced minus "as prepared") of membranes solubilized at pH 7 (dashed line) and pH 3 (solid line). The insets correspond to a zoom of the 500–650 nm part. The spectra were recorded at room temperature.

the α-bands at 562 and 582 nm was observed when comparing pH 7 to pH 3, which suggests that these cytochromes are stable over a broad (acidic) pH range (Fig. 2A and B).

An important fraction of hemes a_{582} and a/a_3 (absorbing at 597 nm) is in a reduced state in the "as prepared" sample, suggesting higher midpoint redox potentials of these two hemes as compared to heme b_{562}, which was oxidized in the "as prepared" samples (Fig. 2). Heme b_{562} is not reduced in the presence of ascorbate (data not shown).

3.3. Cytochrome c oxidase activity of solubilized membranes of F. acidiphilum

The terminal oxidases of certain archaea can oxidize horse heart ferrocytochrome *c* in spite of the fact that these species do not always possess cytochrome *c*. Ferrocytochrome *c* was thus used to measure cytochrome *c* oxidase activity (at pH 5) in *Ferroplasma* membranes solubilized at pH 3 and pH 7. Activity was detected in both samples but was found to be more than double in membranes solubilized at pH 3 as compared to pH 7 (73.0 ± 9 nmol min^{-1} mg^{-1} versus 29.5 ± 8 nmol min^{-1} mg^{-1}, Fig. 3). Complete inhibition of these activities (for both samples) was obtained by 300 μM potassium cyanide, a typical inhibitor of heme copper oxidases. These results confirm the presence of terminal oxidase activity in solubilized membranes and show that the corresponding enzyme is functionally affected when solubilized at neutral pH as compared to an acidic pH.

3.4. Identification of functional respiratory enzymes on Blue native gels

To investigate the presence of electron transfer chain components and to detect potential physical interactions between the solubilized electron transfer proteins, membrane proteins from *Ferroplasma* solubilized at low and neutral pH values were loaded on Blue native (BN) gels. BN gels allow separation of proteins or protein complexes based on their molecular mass while retaining protein interactions and activities [27,48]. After Coomassie Blue staining, five major bands were revealed with apparent masses in the range of 100–1000 kDa, indicating that high molecular mass proteins or complexes were extracted from *Ferroplasma* membranes (Fig. 4, lane 1).

3.4.1. Cytochrome c oxidase

As the preservation of enzyme activity is strongly indicative of native conditions, BN electrophoresis was combined with in-gel cytochrome *c* oxidase activity staining (Fig. 4, lanes 2 and 3). Interestingly, more than one protein band exhibited cytochrome *c* oxidase activity at a priori unexpected apparent molecular masses of around 370 and 850 kDa. This activity represents true cytochrome *c* oxidase since it is inhibited in presence of cyanide (data not shown). The observed masses are higher than usual for classical prokaryotic oxidases, which strongly suggests that this enzyme complex oligomerizes or associates with other proteins in the membranes to form supercomplexes of 850 and 370 kDa. The activity staining band intensities significantly vary according to the pH at which the membranes were solubilized: as compared to pH 7, at pH 3 the activity of the 850 kDa complex decreases whereas the activity of the 370 kDa complex increases (Fig. 4, lanes 2 and 3). It is conceivable that at low pH, the 850 kDa complex dissociates into a smaller form that retains the cytochrome *c* oxidase activity. The activity of the 370 kDa complex from membranes solubilized at pH 7 varied among different purification batches but was often hardly detectable.

3.4.2. Iron oxidase

With the purpose of identifying the enzyme (complex) responsible for the direct oxidation of Fe(II), we have developed a novel method for the detection of iron oxidase activity directly in-gel. This activity can be represented by the overall reaction $Fe(II) + O_2 \leftrightarrow Fe(III) + H_2O$. The enzymes involved in both iron oxidation and oxygen reduction must be physically associated so that electron transfer from Fe(II) to oxygen can occur in the gel band. The formation of Fe(III) oxide precipitate upon enzymatic Fe(II) oxidation serves for activity band detection. Since the abiotic (unspecific) oxidation of Fe(II) is negligible at low pH, the assay was performed at pH 3. As is the case for the cytochrome *c* oxidase activity, we could detect two different bands at around 370 kDa and 850 kDa, although the iron oxidase activity is more intense in the latter (Fig. 4, lanes 4 and 5). Again, the intensity of the bands depends on the pH used for membrane solubilization. Iron oxidase activity was at least partially inhibited by potassium cyanide (not shown), which confirms involvement of a terminal oxidase in the electron transfer detected by this assay. Moreover, similar experiments performed under anaerobic conditions did not yield any activity (data not shown). The fact that the cytochrome *c* oxidase- and the iron oxidase activities colocalize in the gel implies that they are physically and probably functionally associated in the membrane of *Ferroplasma*. It thus seems that the components of the entire respiratory chain are organized in a supramolecular complex.

Given that samples solubilized at pH 3 and pH 7 are similar in terms of specific activity and spectroscopic properties, and that proteins

Table 1
Properties of respiratory complexes found in some acidophilic archaea.

Strains	Respiratory complex	Components Theoretical molecular mass	Hemes	Spectral properties	References
"*Ferroplasma acidarmanus*"	Quinol oxidizing–O_2 reducing complex[a]	Cytochrome b_{562} Rieske iron–sulfur protein Sulfocyanin Putative cbb_3 oxidase		Under chemomixotrophic growth: 596, 583, 437 nm (red)[a] Under chemoorganotrophic growth: 596, 562, 425 nm (red)[a]	[26]
Sulfolobus acidocaldarius	SoxABCD		4 hemes a_S	604–606, 586–587, 440–441 nm (red-ox); 601–605, 586, 435–439 (red)	[17], [19], [23], [24], [36]
	280 kDa (monomeric)	SoxA (subunit II of heme-copper oxidase), 19 kDa	–		
	570 kDa (oligomeric, low salt)	SoxB (subunit I of heme-copper oxidase), 58 kDa	*a*, a_3 (+220, +370 mV)		
		SoxC (cytochrome *b*), 63 kDa	a_{587}, a_{587} (+210, +270 mV)		
		SoxD, 4.5 kDa	–		
	SoxM		2 hemes *as*, 2 hemes *b*	587, 561, 441, 436 nm (red-ox)	[18], [22], [24], [25], [37]
	225 kDa (theoretical, for monomer)	SoxM (subunit I + III of heme-copper oxidase), 88 kDa	*b*, b_3 (+200, +350 mV)		
		SoxH (subunit II of heme-copper oxidase), 16 kDa	–		
		SoxG (cytochrome *b*), 57 kDa	a_{587}, a_{587} (+20–30, +100 mV)		
		SoxF (Rieske iron–sulfur protein), 27 kDa	–		
		SoxE (sulfocyanin), 21 kDa	–		
		SoxI, 17 kDa	–		
	bc-analogous complex[b] (Sox-Cbs)				[38], [39], [40]
		SoxN (cytochrome *b*), 59 kDa SoxL (Rieske iron–sulfur protein), 26 kDa			
		CbsA (monoheme cytochrome $b_{558/566}$), 51 kDa	*b* (> + 350 mV)		
		CbsB, 35 kDa OdsN, 12 kDa			
Sulfolobus tokodaii strain 7	SoxM-like supercomplex		1 heme *b*, 3 hemes a_s	603, 582, 558, 442 nm (red-ox, low-T°)	[20], [21]
		Cytochrome b_{562}	b_{562} (+146 mV)		
		Cytochrome a_{583}	a_{583} (+270 mV)		
		Rieske iron–sulfur protein	–		
		Cytochrome aa_3	*a*, a_3 (+117, +325 mV)		
Acidianus ambivalens	Cytochrome *ba* complex[c] (*bc*-analogous complex, Sox-Cbs)		2 hemes *b*, 1 heme a_s	584, 574, 561 nm (red-ox)	[41]
		SoxN (cytochrome *b*), 62 kDa	*as*, *b* (+160, +200 mV)		
		CbsA (monoheme cytochrome *b*), 46 kDa	*b* (+400 mV)		
		SoxL (Rieske iron–sulfur protein), 35 kDa			
		CbsB, 35 kDa OdsN, 11.5 kDa			
	aa_3 quinol oxidase[d] (Dox)		2 hemes a_s	590, 428 nm (red-ox)	[42], [43], [44], [45], [46]
		DoxB (subunit I of heme-copper oxidase), 65 kDa	*a*, a_3 (+320, +390 mV)		
		DoxC (pseudosubunit II of heme-copper oxidase), 38 kDa			
		DoxE, 7.1 kDa			
		DoxF, 7.2 kDa			

Theoretical molecular masses were taken from references or calculated, when possible, using the tool Compute pI/Mw (http://web.expasy.org/compute_pi/). Red is for reduced; ox is for oxidized.

[a] Predicted complex (not purified). Spectral properties are those of the archaeal membranes.
[b] Predicted complex, only CbsA and SoxL were characterized.
[c] The complex was purified with two subunits only, CbsA and SoxN. This complex may constitute a predicted quinol oxidizing bc_1-analogous complex with CbsB, SoxL and OdsN.
[d] Predicted complex, only DoxB and DoxC were purified.

prepared at pH 7 tend to precipitate with time, further experiments have been performed at pH 3 only.

3.5. Purification and functional characterization of the 850 kDa complex

Since the activity bands observed on BN gels differed significantly in molecular mass, we developed a purification strategy based on this criterion for further characterization of the putative complexes. The solubilized membrane proteins were separated on a 15–40% glycerol density gradient. The gradient was divided into six fractions which were analyzed by optical spectroscopy, BN gel electrophoresis and cytochrome *c* oxidase activity measurements. Typical absorbance signals of heme-copper oxidases (597 nm) were found in fraction 6 (F6), the heaviest fraction at approximately 35–40% glycerol (Fig. 5). Peaks at 562 and 582 nm were found for lighter fractions (mainly F2 and F3 at around 19–26% glycerol). Intermediate fractions (F4 and F5) contained all these components with signals at 597, 582 and 562 nm (Fig. 5). The highest specific cytochrome *c* oxidase activity was found in F6 (Fig. 5),

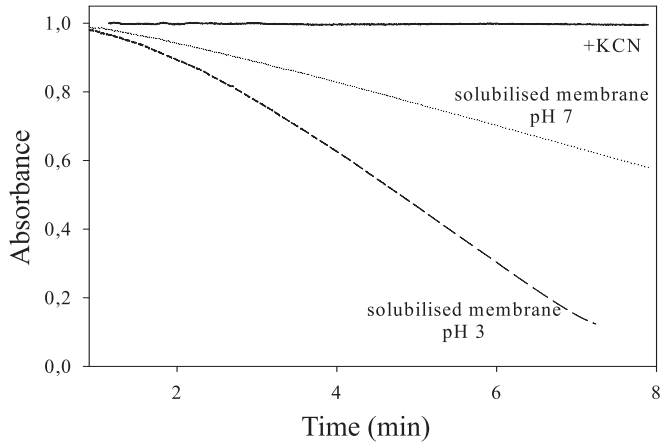

Fig. 3. Oxidation of exogenous ferrocytochrome *c* by *F. acidiphilum* membranes solubilized at pH 3 and 7. Oxidation kinetics of horse heart ferrocytochrome *c* (50 μM), in assay buffer at pH 5, was monitored at 552 nm with 60 μg of sample "as prepared" at pH 7 (dotted line), "as prepared" at pH 3 (dashed line) and with 300 μM KCN (samples prepared at pH 3) (solid line).

which point to the cytochrome *c* oxidase being part of the high molecular weight protein complex. However, F6 (and F5) was found to contain not only the 850 kDa complex but also that of 370 kDa, described above (data not shown). The complexes comprising the cytochrome *c* oxidase signals (F6) and the heme(s) b_{562} and a_{582} signals (fractions F2 and F3) were further purified and characterized. Applying F6 from the density gradient to gel filtration chromatography enabled the complete separation of the large cytochrome *c* oxidase complex (850 kDa) from the smaller one (370 kDa), as shown on BN gels (see below; Fig. 7). Spectroscopic analysis of the further purified 850 kDa complex reveals peaks around 597 and 440 nm (in the reduced state), corresponding to an oxidase. The absence of heme b_{562} indicates that the *F. acidiphilum* terminal oxidase is of the aa_3-type (Fig. 6A). EPR spectra recorded on the purified 850 kDa complex (in the "as prepared" state) at 15 K shows a large signal at g = 6, typical for high-spin hemes (data not shown) and a signal at g = 3.04 that could arise

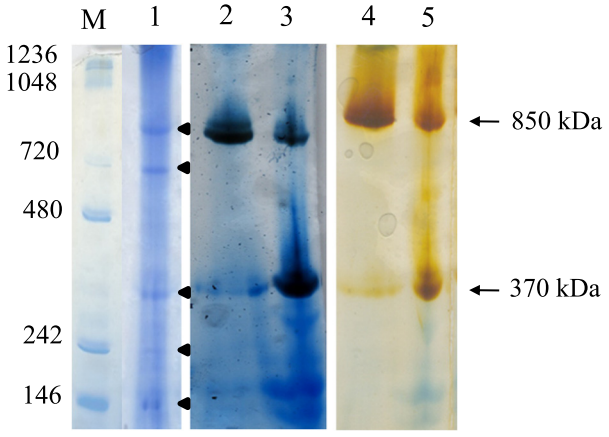

Fig. 4. Analysis of *F. acidiphilum* solubilized membranes on 4–15% Blue-native gels. Separation of pH 7 solubilized membranes stained with Coomassie Blue (lane 1), cytochrome *c* oxidase activity (lane 2), and ferrous iron oxidase activity (lane 4). Separation of pH 3 solubilized membranes stained for cytochrome *c* oxidase activity (lane 3), and ferrous iron oxidase activity (lane 5). Molecular weight markers are indicated in kDa (Lane M). Thirty micrograms of proteins was loaded in each lane. Cytochrome *c* oxidase activity was detected at pH 6.8 and ferrous iron oxidase activity was detected at pH 3.

from the low-spin heme of the cytochrome *c* oxidase catalytic subunit, such as that found in mitochondrial or bacterial terminal oxidases [49–52].

To precisely define its subunit composition, the 850 kDa complex was run both on a denaturing gel and on a BN gel (Fig. 7A, B), whereafter bands were cut out and analyzed by mass spectrometry. Fig. 7B shows the denaturing gel run with solubilized *Ferroplasma* membranes (lane 1) and the 850 kDa complex (lane 2). Mass spectrometry analyses demonstrate the presence of cytochrome *c* oxidase subunits (subunits I + III fused, subunit II) in line with the results from optical spectra (Tables 2, S1 and S2 in Supporting information). Moreover, the complex contains a blue copper protein annotated as sulfocyanin, hitherto found in some archaeal respiratory complexes [24,37]. Genes encoding oxidase subunits and sulfocyanin are found in a single operon in *Ferroplasma* species (Fig. 1D). Interestingly, a small hypothetical protein (about 7300 Da, accession number YP_008142004) of unknown function was also identified (Tables 2, S1 and S2; bands from Fig. 7A) whose gene is located only three genes upstream of that coding for the oxidase subunit I/III in the "*F. acidarmanus*" genome. Since the genome sequence of *F. acidiphilum* is not yet available, genome sequences of close species are used for protein identification. This may account for the fact that the number of unique peptides detected by the mass spectrometry analyses is rather low. However, identification results are considered robust because the same proteins were identified using two distinct types of polyacrylamide gel, two different mass spectrometers as well as different search engines. No *b*-type cytochrome, Rieske protein or other redox proteins were detected in this complex, in accordance with the spectroscopic data.

In-gel enzymatic activities revealed that the purified complex of 850 kDa possesses substantial cytochrome *c* oxidase- and iron oxidase activities (Fig. 7A, lanes 1 and 2 respectively). This was corroborated by both cytochrome *c* oxidase- and iron oxidase specific activity measurements. The cytochrome *c* oxidase activity, specifically inhibited by 300 μM KCN, was found to be around 430 nmol min^{-1} mg^{-1}, which is not high compared to some other cytochrome oxidases. This is likely due to the use of cytochrome *c* as electron donor (not present in *Ferroplasma*) and the pH difference that exists in vivo on either side of the cytoplasmic membrane, which cannot be reproduced in vitro (Fig. 7C). The activity of the high molecular mass complex was confirmed by polarographic oxygen consumption measurements using Fe(II) as electron donor (iron oxidase activity), which yielded the relative high value of 3840 nmol min^{-1} mg^{-1} (Fig. 7C). This confirms that the purified 850 kDa complex contains an iron oxidase and an oxygen reductase, able to transfer electrons from the primary energy source (Fe(II)) to the terminal acceptor (oxygen). However, with Fe(II) as electron donor, the reduction of oxygen cannot be fully inhibited by KCN suggesting that a part of the oxygen is not reduced in the active site of the oxidase (Fig. 7C) but in a non-specific manner, potentially by the sulfocyanin. Moreover, we tried to detect an O_2 consumption using quinol as electron donor (instead of Fe) with the purified large oxidase complex, which gave no activity (data not shown). This seems consistent to us, as this purified complex contains only the sulfocyanin and the aa_3 oxidase, not known to bear a quinol binding site.

3.6. Purification and functional characterization of the 370 kDa complex

As mentioned above, an additional purification step allowed the separation of the 850 kDa from the 370 kDa complex. The BN gel migration profile of the purification fraction containing the smaller complex shows two bands with estimated molecular masses of 370 and 300 kDa (Fig. 7D, lanes 1 and 2). Only the 370 kDa band was revealed by oxidase- and iron oxidase activities, indicating that the smaller protein band (300 kDa, marked with an asterisk in Fig. 7D) is not involved in electron transport from Fe(II) to oxygen. As reported below (see Table S3), this 300 kDa protein was identified as an extracellular solute binding protein. On BN gel, the 370 kDa complex displays cytochrome *c*

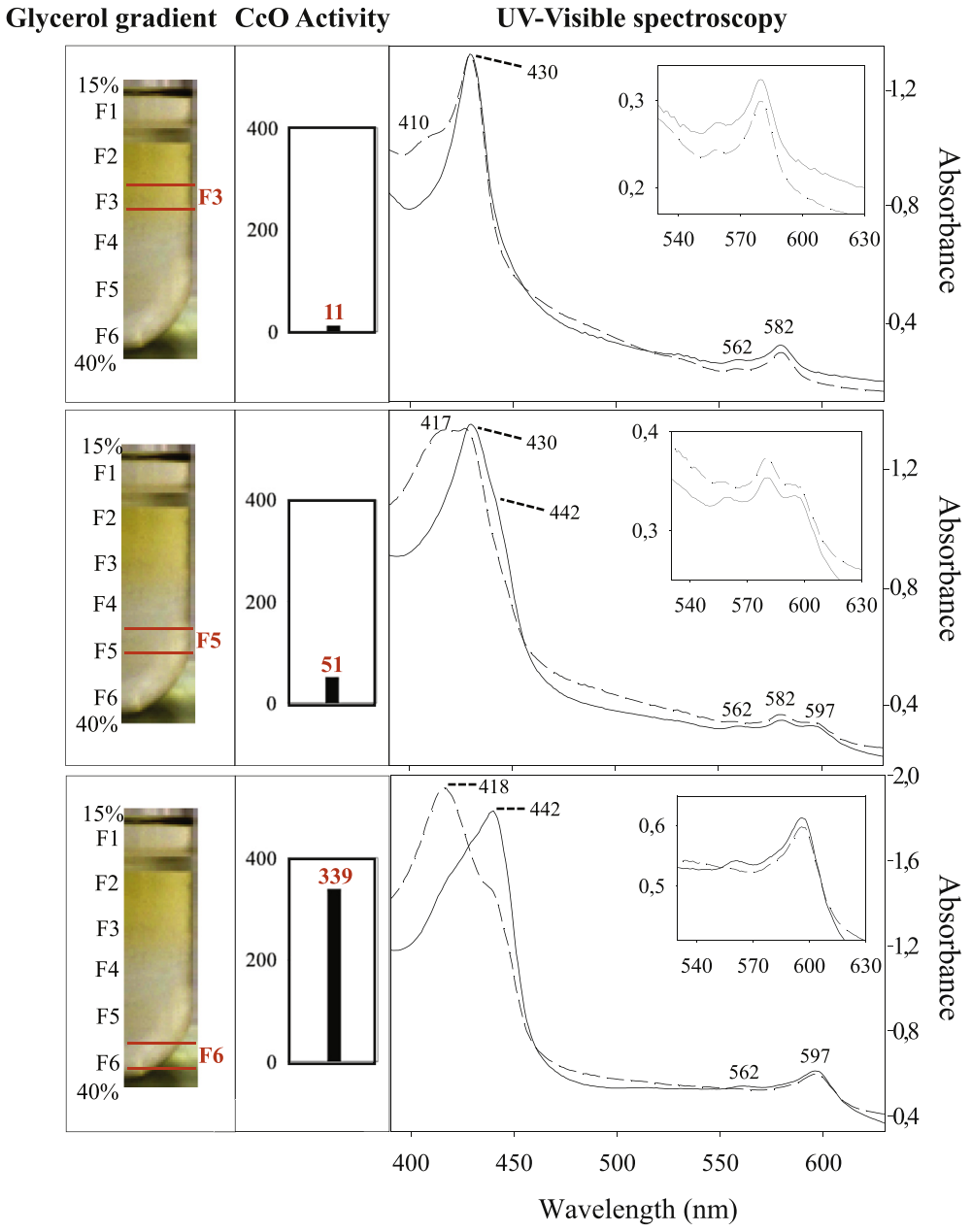

Fig. 5. Cytochrome *c* oxidase activity and absorption spectra of fractions collected from glycerol density gradients. Solubilized membranes at pH 3 were separated on a 15–40% glycerol gradient which was fractionated into six fractions (F1 to F6), as shown on the left. Cytochrome *c* oxidase (CcO) activity and optical spectra are shown for F3, F5 and F6. Activity is expressed as nmol min^{-1} mg^{-1}. Proteins were analyzed by spectroscopy "as prepared" (dashed lines) and reduced by sodium dithionite (solid lines). The insets correspond to a zoom of the 530–630 nm part. The spectra were recorded at room temperature.

oxidase- (Fig. 7D, lane 1) and iron oxidase activity stainings (lane 2) that are much weaker than those of the purified 850 kDa complex (Fig. 7A). This also translates into negligible specific cytochrome *c* oxidase and iron activities (Fig. 7F), suggesting that the 370 kDa complex is destabilized during the purification step.

To determine the subunit composition of the 370 kDa complex, protein bands excised directly from the BN gel or from a two dimensional (2D) BN/SDS gel (Fig. 7D and E) were analyzed by mass spectrometry. The results are summarized in Tables 2, S2 and S3, revealing that the subunit composition of the 370 kDa complex is similar to that of the 850 kDa complex. Moreover, we found that oxidase subunit II and sulfocyanin are detected in the same bands on 2D gel (Fig. 7E spots 2 and 3, Tables 2 and S3). This finding may suggest that these two proteins interact with each other and form a stable subcomplex.

All together these results indicate that *F. acidiphilum* solubilized membranes contain a high molecular weight complex (850 kDa) and a smaller complex (370 kDa) that are both able to reduce molecular oxygen with Fe(II) as electron donor. These complexes are both composed of at least an aa_3-type oxidase and a sulfocyanin, and are encoded by a single operon (Fig. 1D). The 850 kDa complex probably dissociates in vitro into the less active 370 kDa form. This is rationalized by the facts that (i) only one heme copper oxidase operon is found in the genomic sequence of "*F. acidarmanus*" and "*F.* Type II" (Fig. 1D), (ii) the protein composition

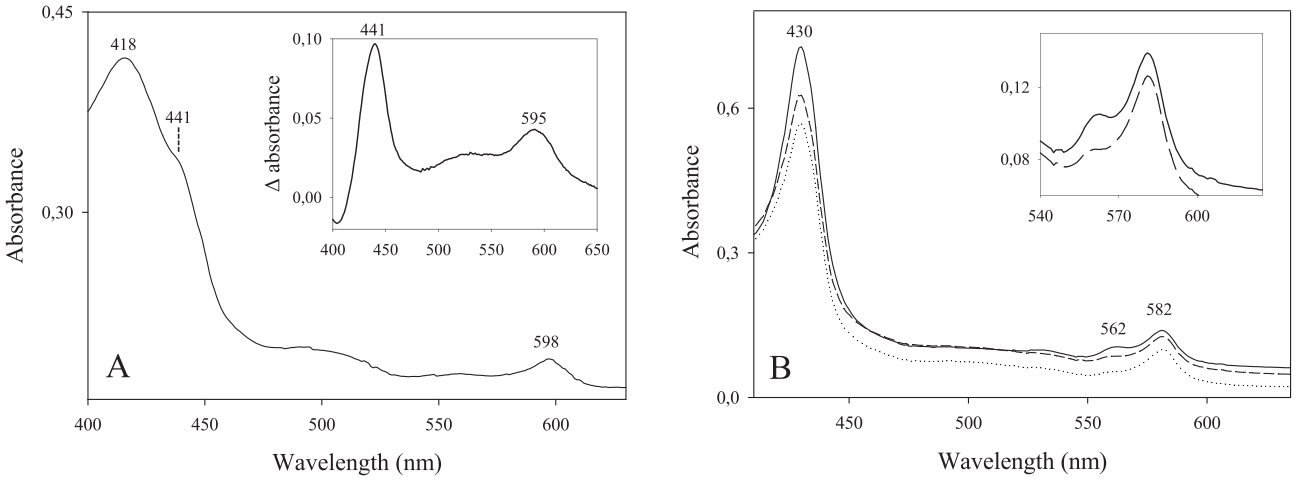

Fig. 6. Absorption spectra of the purified 850 kDa complex and the cytochrome b_{562}–a_{582} complex. A, The 850 kDa complex was analyzed "as prepared". The inset shows the difference spectrum (reduced by sodium dithionite minus "as prepared"). B, The cytochrome *ba* complex was analyzed "as prepared" (dotted line), reduced by sodium ascorbate (dashed line) and reduced by sodium dithionite (solid line). The inset corresponds to a zoom of the 540–620 nm part. The spectra were recorded at room temperature.

and enzymatic activities of the 370 and 850 kDa complexes are the same and that (iii) the 370 kDa complex is not found in all conditions.

3.7. The cytochrome b_{562}–a_{582} complex

As stated above, we also endeavored to purify the complex containing the hemes b_{562} and a_{582}, detected in fractions F2 and F3. These fractions were pooled and further purified on a hydroxyapatite column. The co-purification of both hemes (or cytochromes) suggests their stable association in a complex or in the same protein. As expected, no cytochrome *c* oxidase activity was detected in this fraction, in agreement with the spectroscopic data showing the absence of absorbance peaks typical for a cytochrome *c* oxidase (Fig. 6B). The optical heme b_{562} and a_{582} signals are reminiscent of those obtained for archaeal homologs

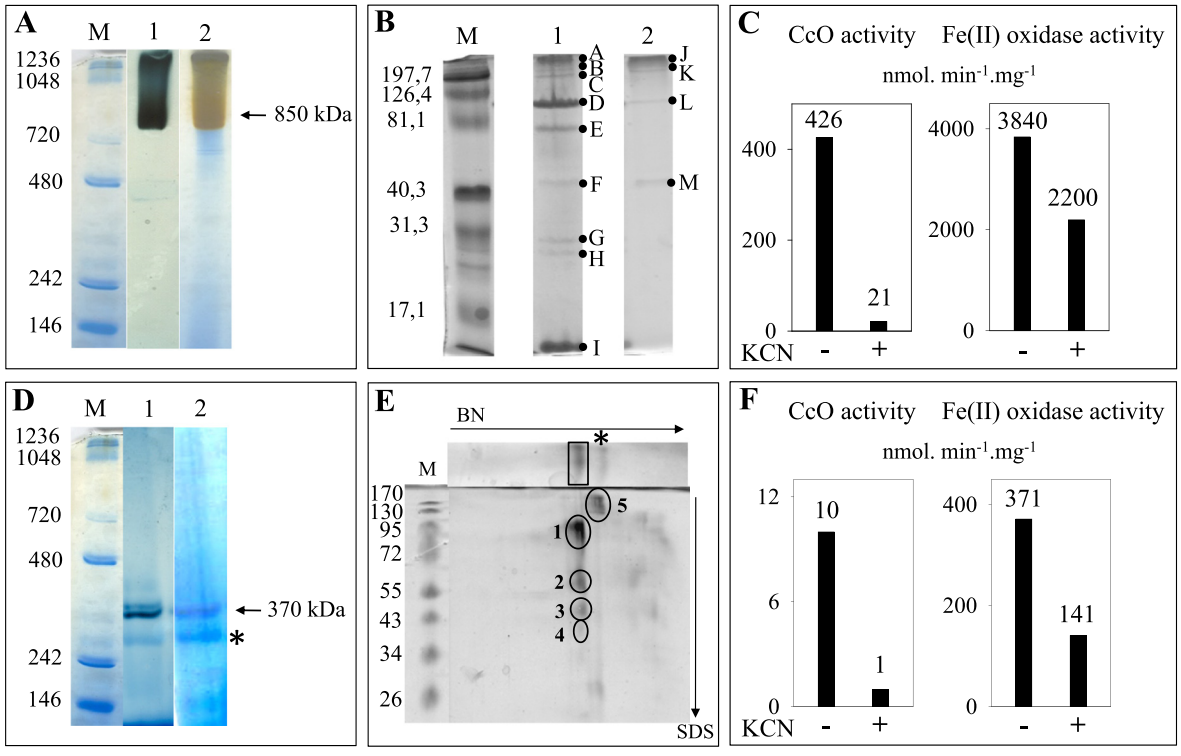

Fig. 7. BN- and denaturing gel analysis of the purified 850- and 370 kDa complexes and their cytochrome *c* oxidase- and iron oxidase activities. A and D, Migration of the 850 kDa complex (panel A) and the 370 kDa complex (panel D) on a 4–15% BN gel stained for cytochrome *c* oxidase activity (lane 1) and ferrous iron oxidase activity (lane 2). Thirty micrograms of proteins was loaded in each lane. B, Migration of *F. acidiphilum* solubilized membrane proteins (lane 1) and the purified 850 kDa complex (50 μg, lane 2) on a 15% SDS gel stained with Coomassie Blue. E, Separation of the purified 370 kDa complex (150 μg) by 2D BN/SDS-PAGE and subsequent Coomassie Blue staining. Molecular weight markers are indicated in kDa on the left (lane M). The band marked with a * (panels D and E) is not detected by any activity and is a contaminant of fractions containing the 370 kDa complex. Bands identified by mass spectrometry are labeled with letters (panel B) or with numbers (panel E). Mass spectrometry identifications are reported in Tables 2, S1, S2 and S3. C and F, Cytochrome *c* oxidase (CcO) and iron oxidase specific activities determined for the purified 850 kDa complex (panel C) and the 370 kDa complex (panel F). Kinetics of oxidation of 50 μM of ferrocytochrome *c* was monitored at 552 nm after addition of 15 μg of proteins. O_2 consumption activity using ferrous iron as electron donor (iron oxidase activity) was determined polarographically. The reactions have been done in the presence or absence of 300 μM KCN. Rates were corrected for the non-enzymatic reaction. All reactions (enzymatic and non-enzymatic) were measured at least in triplicate. Both activities are expressed as nmol min^{-1} mg^{-1}.

Table 2
Summary of subunits of the 850 and 370 kDa complexes identified by mass spectrometry.

Figure	Band	App. Mr	Complex	Protein ID	NCBI entry	Theor. Mr
7A (BN gel)	850 kDa	850	850 kDa	Cytochrome c oxidase polypeptide I/III	YP_008142008	93087
				Sulfocyanin	YP_008142010	22316
				Hypothetical protein	YP_008142004	7294
				Cytochrome c oxidase polypeptide II	YP_008142011	31047
7B (SDS gel)	A, J	>200	850 kDa	Cytochrome c oxidase polypeptide I/III	YP_008142008	93087
	F, M	45	850 kDa	Cytochrome c oxidase polypeptide II	YP_008142011	31047
7D (BN gel)	370 kDa	370	370 kDa	Cytochrome c oxidase polypeptide I/III	YP_008142008	93087
				Sulfocyanin	YP_008142010	22316
				Cytochrome c oxidase polypeptide II	YP_008142011	31047
				Hypothetical protein	YP_008142004	7294
7E (2D gel)	1	95	370 kDa	Cytochrome c oxidase polypeptide I/III	YP_008142008	93087
	2	60	370 kDa	Cytochrome c oxidase polypeptide II	YP_008142011	31047
				Sulfocyanin	YP_008142010	22316
	3	50	370 kDa	Cytochrome c oxidase polypeptide II	YP_008142011	31047
				Sulfocyanin	YP_008142010	22316
	4	40	370 kDa	Cytochrome c oxidase polypeptide II	YP_008142011	31047

Only proteins known or assumed to be involved in energy electron transfer are reported in this table, the totality of identified proteins being reported in Tables S1, S2 and S3 in Supporting information. Details concerning protein identification (predicted function, peptides for identification and organism of the protein candidate) are found in Tables S1, S2 and S3. Table heading: Band, letters and numbers refer to the protein bands from gels shown in Fig. 7; App. Mr, apparent molecular mass (in kDa) of the band estimated on gel; Complex, indicate to which purified complex the identified proteins belong; Protein ID, identity in the National Center for Biotechnology Information (NCBI) database; NCBI entry, accession number; Theor. Mr, theoretical molecular mass of the protein in Da (from NCBI). Bands cut out from gels in Fig. 7A and D were detected with the cytochrome *c* oxidase activity (lane 1).

of cytochrome *b* of the Rieske–cytochrome *b* complex (e.g. the di-heme cytochrome SoxN subunit of the *bc*-analogous complex of the acidophilic archaeon *A. ambivalens* is proposed to harbor a heme *b* and a heme a_s), or of the *Sulfolobus* SoxM complexes [20,24,41] (Table 1 and Fig. S1). This cytochrome b_{562}–a_{582} complex is thus likely encoded by the "cytochrome *b*–Rieske protein" operon in *Ferroplasma* (Fig. 1A, [16]). In "*F. acidarmanus*" and "*F.* Type II", the di-heme cytochrome seems to possess transmembrane helices and conserved heme binding residues, whereas the Rieske protein exhibits typical iron–sulfur cluster-binding residues [41].

To establish whether these proteins (Rieske protein and cytochrome *b*) are indeed present, the enriched fraction was run on denaturing or native gels and bands of interest were cut out and analyzed by ion trap mass spectrometry (data not shown).

Cytochrome *b* could not be identified in the *Ferroplasma* samples by mass spectrometry, for several reasons: (i) as already mentioned, the genome of *F. acidiphilum* is not yet available and mass spectrometry data are only searched against sequenced genomes, (ii) for protein identification, only 23% of "*F.* Type II" cytochrome *b* sequence is covered by theoretical tryptic peptides accurately detectable by mass spectrometry (meaning that at least 77% of the sequence is theoretically undetectable by this technique), and (iii) cytochrome *b* is a highly hydrophobic protein with numerous transmembrane helices providing a tryptic peptide map fingerprint not favorable for mass spectrometry detection (large and hydrophobic peptides) [27]. Attempts to detect this protein with the specific heme-staining protocol using 3,3′,5,5′-tetramethylbenzidine in denaturing gels without reducing agent were unsuccessful; however the presence of heme-containing proteins in the sample was confirmed by an intense staining at the gel migration front, corresponding to free hemes.

The Rieske iron–sulfur protein could be identified in bands at a molecular mass of around 35 kDa on SDS gel and 150 kDa on BN gel (data not shown). This protein was unambiguously identified via two unique peptides (Fig. S2). Rieske proteins in acidophilic archaea ("*Ferroplasma* type II", *T. volcanium*, *A. ambivalens*, *S. acidocaldarius*, *P. torridus*) vary in molecular mass from 25 to 35 kDa. The fact that the Rieske protein of *F. acidiphilum* was present in a gel band at roughly 35 kDa indicates that its molecular mass is similar to those of its close homologs.

Although the complex could not be purified to homogeneity, several arguments favor the presence of a Rieske–cytochrome *b*-type complex in the membrane of *F. acidiphilum*: (i) co-purification of hemes with optical signals at 562 and 582 nm suggests the presence of hemes *b* and *a*, already described for archaeal counterparts of the bc_1 complex of bacteria and eukarya; (ii) presence of the Rieske iron–sulfur protein demonstrated by mass spectrometry; and (iii) the theoretical molecular mass of the complex (150 kDa) matched that found on BN gel.

4. Discussion

Here we report a detailed analysis of the respiratory complexes involved in archaeal iron oxidation, an essential process in many natural and man-made acidophilic environments. We showed that *F. acidiphilum* contains a membrane-bound high molecular mass protein complex which comprises an aa_3-type oxygen reductase and a sulfocyanin copper protein, able to oxidize ferrous iron and reduce molecular oxygen, thus providing energy to sustain life. In addition, we found a second membrane electron transfer complex that is a putative homolog of a Rieske/cytochrome *b*-like complex (cytochrome *ba* complex). Speculative models proposed for the electron transfer chains in "*F. acidarmanus*" and "*F.* Type II" involve a SoxM-like supercomplex, associating elements from both Rieske–cytochrome *b* complexes and terminal oxidases [16–26] (Figs. 1 and S1). In our conditions, the biochemical results we obtained do not indicate the presence of a SoxM-type supercomplex in the membrane of *F. acidiphilum*, but rather the presence of two separate complexes, encoded by two different operons (Fig. 1A and D).

The purified 850 kDa complex harbors all the necessary constituents for the entire Fe(II) oxidation–oxygen reduction pathway. Arranged into a functional structure, it thus constitutes a complete and stable respirasome. This multienzyme complex is schematized in Fig. 8. We propose that the sulfocyanin, which tightly associates with oxidase subunit II (Table S3), is the primary electron acceptor from Fe(II) and as such directly interacts with the energy source at the surface of the cells. A Fe(II)-oxidizing role of sulfocyanin was previously proposed for "*F. acidarmanus*" [26] (Fig. S1). The unusually strong association of a small copper protein with an oxidase was also described for *A. ferrooxidans* in the form of a stable complex between the cupredoxin AcoP and the aa_3 cytochrome *c* oxidase [53,54].

The very high apparent molecular mass of the oxidase complex might indicate an oligomerization of certain components. The supramolecular organization of proteins involved in electron transfer chains could improve the stability of the system and optimize the electron transfer. Indeed, *Ferroplasma* is able to grow in an extreme environment

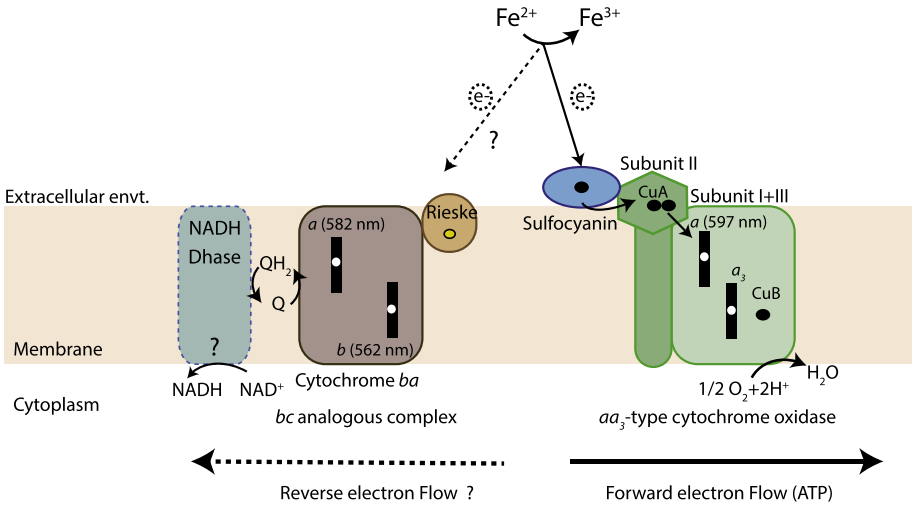

Fig. 8. Tentative model of the Fe(II) oxidation pathways in *F. acidiphilum*. The forward electron flow (or downhill pathway) involves the sulfocyanin and the aa_3-type heme-copper oxidase, whereas the putative proton motive force-dependent reverse electron flow (or uphill pathway) might be constituted by a complex homologous to a Rieske/cytochrome *b*-type complex and a putative NADH dehydrogenase (NADH Dhase). ATP synthase produces ATP while using the proton motive force created by the electron transport chain. Hemes are represented by circles within bars, the [Fe–S] cluster by a yellow circle and copper atoms by black circles. Arrows indicate electron transfer. Q, quinone; QH_2, quinol; envt., environment. See text for more details.

with a very poor energy substrate; this spatial arrangement of proteins in the membranes might be a way to overcome these bioenergetics obstacles. In the Fe(II) oxidizing bacterium *A. ferrooxidans*, the aerobic respiratory chain is also organized in a supramolecular structure, but the components are not the same [4]. As numerous species of archaea have been reported to contain proteins bearing glycan moieties, in particular at the cell surface [55], the possibility of glycosylation of proteins of the 850 kDa complex should be considered as an alternative explanation for its very high molecular weight [56,57]. N-glycosylation of proteins may contribute to the ability of archaeal species to survive and adapt to harsh environments [55].

Here, we hypothesize the existence in *F. acidiphilum* of two electron transfer chains that use Fe(II) as initial electron donor, depicted in Fig. 8: the so-called downhill electron pathway (oxygen reduction) dedicated to energy conservation in the cell, and the uphill electron pathway, enabling the regeneration of reducing power (synthesis of NAD(P)H). These two branches of iron oxidation have been well-described in the best-studied iron oxidizer *A. ferrooxidans* [5,8], but are also operating in other chemolithoautotrophic micro-organisms that use inorganic energy sources that are significantly less reducing than NAD(P)H. The uphill pathway is thermodynamically unfavorable if one just considers the redox potential of Fe(III)/Fe(II) and NAD/NADH, but chemiosmotically coupled to the downhill pathway it will become possible. NADH is required for cellular anabolic processes such as the reduction (fixation) of inorganic carbon, essential for autotrophic growth. We suggest that in *F. acidiphilum*, the Rieske/cytochrome *ba* complex is involved in this proton-motive force-driven reverse electron transport chain, as described for *A. ferrooxidans* [5] and also recently hypothesized to operate in the thermoacidophilic iron-oxidizing archaeon *M. yellowstonensis* [31]. A putative NADH dehydrogenase is likely present in the membrane of *F. acidiphilum* to receive electrons from the quinone pool and reduce NAD(P). Interestingly, an operon encoding a complex homologous to the bacterial complex I is found in the genome of "*F. acidarmanus*", but the three subunits responsible for NADH binding and oxidation are lacking, which is typical in archaea. Further biochemical studies should identify the NADH dehydrogenase in this archaeon.

Acidophilic iron oxidizers have been identified not only in archaea but also among bacteria. Even though some of them live in the same habitats, micro-organisms have clearly different ferrous iron respiratory chains, including heterogeneities of the terminal heme copper oxidases and the direct iron oxidase proteins (reviewed in [8]). The present study confirms that the electron carriers of iron pathways are clearly dissimilar from one species to another, even among bioleaching archaea [8]. Indeed, Fox and Sox-Cbs contribute to the dissimilatory oxidation of iron in *Sulfolobales* while different heme copper oxidase and *bc*-analogous complexes are involved in this pathway in the *Thermoplasmatales*. The same likely holds true for neutral pH Fe-oxidizers [9].

The work presented in this study suggests that, in *Ferroplasma*, two routes of electron transport operate from iron, the sulfocyanin being the putative direct oxidant of Fe(II). This assumption, awaiting further verification, implies that very different metallo-proteins (SoxE copper protein, FoxCD cytochrome *b* or cytochrome *c* in bacteria) catalyze the same reaction.

Supplementary data to this article can be found online at http://dx.doi.org/10.1016/j.bbabio.2015.04.006.

Transparency Document

The transparency document associated with this article can be found, in the online version.

Acknowledgments

We thank Dr. Marianne Ilbert, Dr. Elisabeth Lojou and Dr. Maria Luz Cardenas (Laboratoire de Bioénergétique et Ingénierie des Protéines, CNRS, Marseille) for helpful discussions and Robert van Lis (Biospector) for helpful discussions and English correction. The Proteomic Platform of the Mediterranean Institute of Microbiology (IMM) is part of MaP (Marseille Protéomique, IBiSA). Funding was provided by ANR (Agence Nationale de la Recherche, ANR-11-IDEX-0001-02) and by the CNRS (Centre National de la Recherche Scientifique). Cindy Castelle and Magali Roger had a fellowship of the French Ministry of Research (Ministère de l'Enseignement Supérieur et de la Recherche).

References

[1] K.J. Edwards, P.L. Bond, T.M. Gihring, J.F. Banfield, An archaeal iron-oxidizing extreme acidophile important in acid mine drainage, Science 287 (2000) 1796–1799.
[2] P.H. Kinnunen, W.J. Robertson, J.J. Plumb, J.A. Gibson, P.D. Nichols, P.D. Franzmann, J.A. Puhakka, The isolation and use of iron-oxidizing, moderately thermophilic acidophiles from the Collie coal mine for the generation of ferric iron leaching solution, Appl. Microbiol. Biotechnol. 60 (2003) 748–753.

[3] T. Rohwerder, T. Gehrke, K. Kinzler, W. Sand, Bioleaching review part A: progress in bioleaching: fundamentals and mechanisms of bacterial metal sulfide oxidation, Appl. Microbiol. Biotechnol. 63 (2003) 239–248.

[4] C. Castelle, M. Guiral, G. Malarte, F. Ledgham, G. Leroy, M. Brugna, M.T. Giudici-Orticoni, A new iron-oxidizing/O_2-reducing supercomplex spanning both inner and outer membranes, isolated from the extreme acidophile *Acidithiobacillus ferrooxidans*, J. Biol. Chem. 283 (2008) 25803–25811.

[5] S.J. Ferguson, W.J. Ingledew, Energetic problems faced by micro-organisms growing or surviving on parsimonious energy sources and at acidic pH: I. *Acidithiobacillus ferrooxidans* as a paradigm, Biochim. Biophys. Acta 1777 (12) (2008) 1471–1479.

[6] M. Roger, C. Castelle, M. Guiral, P. Infossi, E. Lojou, M.T. Giudici-Orticoni, M. Ilbert, Mineral respiration under extreme acidic conditions: from a supramolecular organization to a molecular adaptation in *Acidithiobacillus ferrooxidans*, Biochem. Soc. Trans. 40 (2012) 1324–1329.

[7] V. Bonnefoy, D.S. Holmes, Genomic insights into microbial iron oxidation and iron uptake strategies in extremely acidic environments, Environ. Microbiol. 14 (2012) 1597–1611.

[8] M. Ilbert, V. Bonnefoy, Insight into the evolution of the iron oxidation pathways, Biochim. Biophys. Acta 1827 (2013) 161–175.

[9] D. Emerson, Biogeochemistry and microbiology of microaerobic Fe(II) oxidation, Biochem. Soc. Trans. 40 (2012) 1211-1216.

[10] O.V. Golyshina, K.N. Timmis, *Ferroplasma* and relatives, recently discovered cell wall-lacking archaea making a living in extremely acid, heavy metal-rich environments, Environ. Microbiol. 7 (2005) 1277–1288.

[11] O.V. Golyshina, Environmental, biogeographic, and biochemical patterns of archaea of the family *Ferroplasmaceae*, Appl. Environ. Microbiol. 77 (2011) 5071–5078.

[12] O.V. Golyshina, T.A. Pivovarova, G.I. Karavaiko, T.F. Kondrateva, E.R. Moore, W.R. Abraham, H. Lünsdorf, K.N. Timmis, M.M. Yakimov, P.N. Golyshin, *Ferroplasma acidiphilum* gen. nov., sp. nov., an acidophilic, autotrophic, ferrous-iron-oxidizing, cell-wall-lacking, mesophilic member of the Ferroplasmaceae fam. nov., comprising a distinct lineage of the Archaea, Int. J. Syst. Evol. Microbiol. 50 (Pt 3) (2000) 997–1006.

[13] M. Dopson, C. Baker-Austin, A. Hind, J.P. Bowman, P.L. Bond, Characterization of *Ferroplasma* isolates and *Ferroplasma acidarmanus* sp. nov., extreme acidophiles from acid mine drainage and industrial bioleaching environments, Appl. Environ. Microbiol. 70 (2004) 2079–2088.

[14] H. Zhou, R. Zhang, P. Hu, W. Zeng, Y. Xie, C. Wu, G. Qiu, Isolation and characterization of *Ferroplasma thermophilum* sp. nov., a novel extremely acidophilic, moderately thermophilic archaeon and its role in bioleaching of chalcopyrite, J. Appl. Microbiol. 105 (2008) 591–601.

[15] E.E. Allen, G.W. Tyson, R.J. Whitaker, J.C. Detter, P.M. Richardson, J.F. Banfield, Genome dynamics in a natural archaeal population, Proc. Natl. Acad. Sci. U. S. A. 104 (2007) 1883–1888.

[16] G.W. Tyson, J. Chapman, P. Hugenholtz, E.E. Allen, R.J. Ram, P.M. Richardson, V.V. Solovyev, E.M. Rubin, D.S. Rokhsar, J.F. Banfield, Community structure and metabolism through reconstruction of microbial genomes from the environment, Nature 428 (2004) 37–43.

[17] M. Lübben, B. Kolmerer, M. Saraste, An archaebacterial terminal oxidase combines core structures of two mitochondrial respiratory complexes, EMBO J. 11 (1992) 805–812.

[18] M. Lübben, S. Arnaud, J. Castresana, A. Warne, S.P. Albracht, M. Saraste, A second terminal oxidase in *Sulfolobus acidocaldarius*, Eur. J. Biochem. 224 (1994) 151–159.

[19] M. Lübben, A. Warne, S.P. Albracht, M. Saraste, The purified SoxABCD quinol oxidase complex of *Sulfolobus acidocaldarius* contains a novel haem, Mol. Microbiol. 13 (1994) 327–335.

[20] T. Iwasaki, K. Matsuura, T. Oshima, Resolution of the aerobic respiratory system of the thermoacidophilic archaeon, *Sulfolobus* sp. strain 7. I. The archaeal terminal oxidase supercomplex is a functional fusion of respiratory complexes III and IV with no *c*-type cytochromes, J. Biol. Chem. 270 (1995) 30881–30892.

[21] T. Iwasaki, T. Wakagi, Y. Isogai, T. Iizuka, T. Oshima, Resolution of the aerobic respiratory system of the thermoacidophilic archaeon, *Sulfolobus* sp. strain 7. II. Characterization of the archaeal terminal oxidase subcomplexes and implication for the intramolecular electron transfer, J. Biol. Chem. 270 (1995) 30893–30901.

[22] J. Castresana, M. Lübben, M. Saraste, New archaebacterial genes coding for redox proteins: implications for the evolution of aerobic metabolism, J. Mol. Biol. 250 (1995) 202–210.

[23] M. Gleissner, U. Kaiser, E. Antonopoulos, G. Schäfer, The archaeal SoxABCD complex is a proton pump in *Sulfolobus acidocaldarius*, J. Biol. Chem. 272 (1997) 8417–8426.

[24] G. Schäfer, M. Engelhard, V. Müller, Bioenergetics of the Archaea, Microbiol. Mol. Biol. Rev. 63 (1999) 570–620.

[25] L. Komorowski, W. Verheyen, G. Schäfer, The archaeal respiratory supercomplex SoxM from *S. acidocaldarius* combines features of quinole and cytochrome *c* oxidases, Biol. Chem. 383 (2002) 1791–1799.

[26] M. Dopson, C. Baker-Austin, P.L. Bond, Analysis of differential protein expression during growth states of *Ferroplasma* strains and insights into electron transport for iron oxidation, Microbiology 151 (2005) 4127–4137.

[27] M. Guiral, L. Prunetti, S. Lignon, R. Lebrun, D. Moinier, M.T. Giudici-Orticoni, New insights into the respiratory chains of the chemolithoautotrophic and hyperthermophilic bacterium *Aquifex aeolicus*, J. Proteome Res. 8 (2009) 1717–1730.

[28] M. Kearse, R. Moir, A. Wilson, S. Stones-Havas, M. Cheung, S. Sturrock, S. Buxton, A. Cooper, S. Markowitz, C. Duran, T. Thierer, B. Ashton, P. Meintjes, A. Drummond, Geneious Basic: an integrated and extendable desktop software platform for the organization and analysis of sequence data, Bioinformatics 28 (2012) 1647–1649.

[29] F.L. Sousa, R.J. Alves, M.A. Ribeiro, J.B. Pereira-Leal, M. Teixeira, M.M. Pereira, The superfamily of heme-copper oxygen reductases: types and evolutionary considerations, Biochim. Biophys. Acta 1817 (4) (2012) 629–637.

[30] A.P. Yelton, L.R. Comolli, N.B. Justice, C. Castelle, V.J. Denef, B.C. Thomas, J.F. Banfield, Comparative genomics in acid mine drainage biofilm communities reveals metabolic and structural differentiation of co-occurring archaea, BMC Genomics 14 (2013) 485.

[31] M.A. Kozubal, M. Dlakic, R.E. Macur, W.P. Inskeep, Terminal oxidase diversity and function in "*Metallosphaera yellowstonensis*": gene expression and protein modeling suggest mechanisms of Fe(II) oxidation in the sulfolobales, Appl. Environ. Microbiol. 77 (2011) 1844–1853.

[32] S. Bathe, P.R. Norris, Ferrous iron- and sulfur-induced genes in *Sulfolobus metallicus*, Appl. Environ. Microbiol. 73 (2007) 2491–2497.

[33] Y. Jiao, D.K. Newman, The *pio* operon is essential for phototrophic Fe(II) oxidation in *Rhodopseudomonas palustris* TIE-1, J. Bacteriol. 189 (5) (2007) 1765–1773.

[34] J. Hemp, R.B. Gennis, Diversity of the heme-copper superfamily in archaea: insights from genomics and structural modeling, Results Probl. Cell Differ. 45 (2008) 1–31.

[35] O.V. Golyshina, P.N. Golyshin, K.N. Timmis, M. Ferrer, The 'pH optimum anomaly' of intracellular enzymes of *Ferroplasma acidiphilum*, Environ. Microbiol. 8 (2006) 416–425.

[36] S. Anemüller, G. Schäfer, Cytochrome aa_3 from *Sulfolobus acidocaldarius*. A single-subunit, quinol-oxidizing archaebacterial terminal oxidase, Eur. J. Biochem. 191 (1990) 297–305.

[37] L. Komorowski, G. Schäfer, Sulfocyanin and subunit II, two copper proteins with novel features, provide new insight into the archaeal SoxM oxidase supercomplex, FEBS Lett. 487 (2001) 351–355.

[38] T. Hettmann, C.L. Schmidt, S. Anemüller, U. Zähringer, H. Moll, A. Petersen, G. Schäfer, Cytochrome *b*558/566 from the archaeon *Sulfolobus acidocaldarius*. A novel highly glycosylated, membrane-bound b-type hemoprotein, J. Biol. Chem. 273 (20) (1998) 12032–12040.

[39] B. Schoepp-Cothenet, M. Schütz, F. Baymann, M. Brugna, W. Nitschke, H. Myllykallio, C. Schmidt, The membrane-extrinsic domain of cytochrome *b*(558/566) from the archaeon *Sulfolobus acidocaldarius* performs pivoting movements with respect to the membrane surface, FEBS Lett. 487 (3) (2001) 372–376.

[40] A. Hiller, T. Henninger, G. Schäfer, C.L. Schmidt, New genes encoding subunits of a cytochrome bc_1-analogous complex in the respiratory chain of the hyperthermoacidophilic crenarchaeon *Sulfolobus acidocaldarius*, J. Bioenerg. Biomembr. 35 (2) (2003) 121–131.

[41] T.M. Bandeiras, P.N. Refojo, S. Todorovic, D.H. Murgida, P. Hildebrandt, C. Bauer, M.M. Pereira, A. Kletzin, M. Teixeira, The cytochrome *ba* complex from the thermoacidophilic crenarchaeote *Acidianus ambivalens* is an analog of bc_1 complexes, Biochim. Biophys. Acta 1787 (2009) 37–45.

[42] G. Schäfer, Bioenergetics of the archaebacterium *Sulfolobus*, Biochim. Biophys. Acta 1277 (3) (1996) 163–200.

[43] W.G. Purschke, C.L. Schmidt, A. Petersen, G. Schäfer, The terminal quinol oxidase of the hyperthermophilic archaeon *Acidianus ambivalens* exhibits a novel subunit structure and gene organization, J. Bacteriol. 179 (1997) 1344–1353.

[44] T.K. Das, C.M. Gomes, T.M. Bandeiras, M.M. Pereira, M. Teixeira, D.L. Rousseau, Active site structure of the aa3 quinol oxidase of *Acidianus ambivalens*, Biochim. Biophys. Acta 1655 (1–3) (2004) 306–320.

[45] F.H. Müller, T.M. Bandeiras, T. Urich, M. Teixeira, C.M. Gomes, A. Kletzin, Coupling of the pathway of sulphur oxidation to dioxygen reduction: characterization of a novel membrane-bound thiosulphate:quinone oxidoreductase, Mol. Microbiol. 53 (4) (2004) 1147–1160.

[46] S. Todorovic, M.M. Pereira, T.M. Bandeiras, M. Teixeira, P. Hildebrandt, D.H. Murgida, Midpoint potentials of hemes *a* and a_3 in the quinol oxidase from *Acidianus ambivalens* are inverted, J. Am. Chem. Soc. 127 (39) (2005) 13561–13566.

[47] M. Tanaka, N. Ogawa, K. Ihara, Y. Sugiyama, Y. Mukohata, Cytochrome aa_3 in *Haloferax volcanii*, J. Bacteriol. 184 (2002) 840–845.

[48] H. Schägger, W.A. Cramer, G. von Jagow, Analysis of molecular masses and oligomeric states of protein complexes by blue native electrophoresis and isolation of membrane protein complexes by two-dimensional native electrophoresis, Anal. Biochem. 217 (1994) 220–230.

[49] B.F. Van Gelder, H. Beinert, Studies of the heme components of cytochrome *c* oxidase by EPR spectroscopy, Biochim. Biophys. Acta 189 (1969) 1–24.

[50] J.A. Fee, M.G. Choc, K.L. Findling, R. Lorence, T. Yoshida, Properties of a copper-containing cytochrome c_1aa_3 complex: a terminal oxidase of the extreme thermophile *Thermus thermophilus* HB8, Proc. Natl. Acad. Sci. U. S. A. 77 (1980) 147–151.

[51] N. Sone, A. Naqui, C. Kumar, B. Chance, Pulsed cytochrome *c* oxidase from the thermophilic bacterium PS3, Biochem. J. 223 (1984) 809–813.

[52] A.A. Dispirito, J.D. Lipscomb, A.B. Hooper, Cytochrome aa_3 from *Nitrosomonas europaea*, J. Biol. Chem. 261 (1986) 17048–17056.

[53] C. Castelle, M. Ilbert, P. Infossi, G. Leroy, M.T. Giudici-Orticoni, An unconventional copper protein required for cytochrome *c* oxidase respiratory function under extreme acidic conditions, J. Biol. Chem. 285 (2010) 21519–21525.

[54] M. Roger, F. Biaso, C.J. Castelle, M. Bauzan, F. Chaspoul, E. Lojou, G. Sciara, S. Caffarri, M.T. Giudici-Orticoni, M. Ilbert, Spectroscopic characterization of a green copper site in a single-domain cupredoxin, PLoS One 9 (6) (2014) e98941.

[55] D. Calo, L. Kaminski, J. Eichler, Protein glycosylation in Archaea: sweet and extreme, Glycobiology 20 (2010) 1065–1076.

[56] U. Zahringer, H. Moll, T. Hettmann, Y.A. Knirel, G. Schäfer, Cytochrome $b_{558/566}$ from the archaeon *Sulfolobus acidocaldarius* has a unique Asn-linked highly branched hexasaccharide chain containing 6-sulfoquinovose, Eur. J. Biochem. 267 (2000) 4144–4149.

[57] S. Uthandi, B. Saad, M.A. Humbard, J.A. Maupin-Furlow, LccA, an archaeal laccase secreted as a highly stable glycoprotein into the extracellular medium by *Haloferax volcanii*, Appl. Environ. Microbiol. 76 (2010) 733–743.